ELSEVIER

Surface Science 451 (2000) 1–6

surface science

www.elsevier.nl/locate/susc

Charge-transfer dynamics in slow atom–surface collisions: a new close-coupling approach including continuum discretization

B. Bahrim [a,*], U. Thumm [a,b,1]

[a] *J.R. Macdonald Laboratory, Department of Physics, Kansas State University, Manhattan, KS 66506, USA*
[b] *Institute for Theoretical Atomic and Molecular Physics, Harvard–Smithsonian Center for Astrophysics, 60 Garden Street, Cambridge, MA 02138, USA*

Received 23 July 1999; accepted for publication 11 November 1999

Abstract

Within a new two-center close-coupling expansion, we solve the time-dependent Schrödinger equation for an active electron interacting with a slow projectile and a metal surface. The continuum of conduction-band states corresponding to the motion of the active electron in the metal subspace along the surface normal is discretized in terms of wave packets. Results for the time evolution of the atomic and metallic population amplitudes for an excited hydrogen atom near an aluminum surface are shown and discussed. © 2000 Elsevier Science B.V. All rights reserved.

Keywords: Ab initio quantum chemical methods and calculations; Ion–solid interactions; Jellium models

1. Introduction

The interaction of an atom with a metal surface perturbs the continuum of conduction-band states of the metal and may lead to the transfer of electrons between the two interacting systems. Over the past decade, much experimental and theoretical work has been devoted to the study of charge transfer in atom–surface interactions, including the recent development of non-perturbative methods [1–10]. In this paper, we rewrite the time-dependent Schrödinger equation for an active electron interacting with a metal surface and a slowly moving projectile as a system of coupled differential equations and solve this system numerically. In contrast to other close-coupling approaches [3,5–8,10], we discretize the active electron's motion inside the metal using Weyl wave packets. These stationary wave packets are obtained by the superposition of jellium wavefunctions within a small momentum interval. Their use presents two important advantages. In contrast to jellium states, they are localized in the region near and in the surface, where electronic interactions mainly occur (Fig. 1). On the other hand, the use of discretized states to represent the conduction-band (and possibly the ionization) continuum allows for the convenient inclusion of one-electron transitions inside the substrate, due to the time-dependent perturbation introduced by the moving atom. The couplings between metal states influence the electron transfer between atom and surface.

We assume a classical trajectory to describe the

* Corresponding author.
E-mail addresses: bahrimb@phys.ksu.edu (B. Bahrim), thumm@phys.ksu.edu (U. Thumm)
[1] Also corresponding author.

0039-6028/00/$ - see front matter © 2000 Elsevier Science B.V. All rights reserved.
PII: S0039-6028(00)00002-9

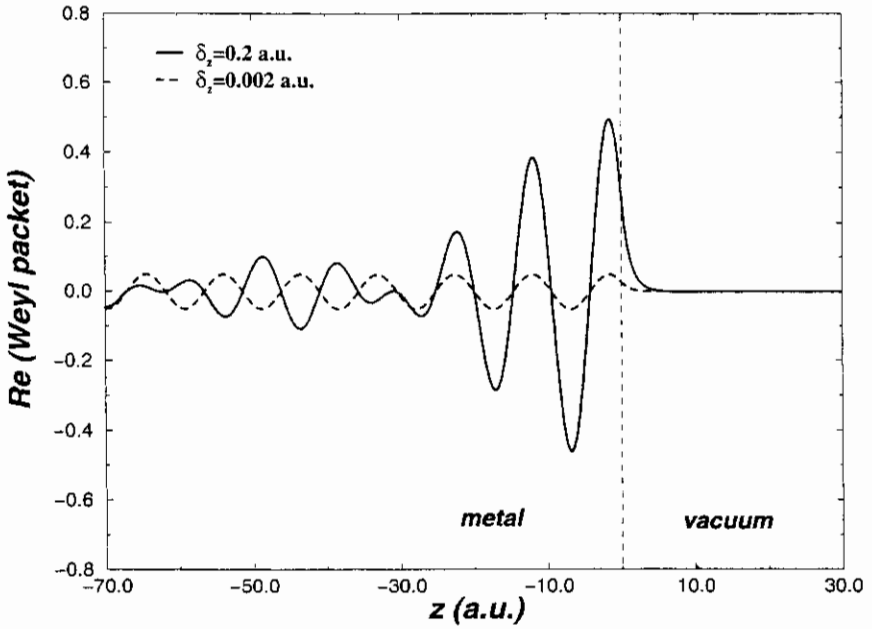

Fig. 1. Real part of two Weyl wave packets as a function of the electron–surface distance z. The wave packets are obtained by superimposing jellium wavefunctions in momentum intervals of widths $\delta_z=0.2$ a.u. and 0.002 a.u., respectively, and are centered around the electron momentum $\bar{k}_z=0.6$ a.u.

perpendicular incidence and reflection of the projectile at the surface. Throughout this paper, distances and electronic energies will be measured with respect to the jellium edge and the atomic ionization threshold, respectively. Our quantization axis is oriented along the surface normal, passing through the center of the atom and pointing away from the surface.

2. Close-coupling theory with continuum discretization

We solve the time-dependent Schrödinger equation by expanding the total one-electron wavefunction as

$$\psi(\boldsymbol{r},t)=\sum_j a_j(t)\exp(-\mathrm{i}E_j t)\psi_j[\boldsymbol{r},\boldsymbol{D}(t)] + \int b_{\boldsymbol{k}}(t)\exp(-\mathrm{i}E_{\boldsymbol{k}}t)\phi_{\boldsymbol{k}}(\boldsymbol{r})\rho_{\boldsymbol{k}}\,\mathrm{d}\boldsymbol{k}, \qquad (1)$$

where ψ_j are the hydrogenic wavefunctions centered on the projectile, and $\phi_{\boldsymbol{k}}$ are the metallic wavefunctions centered on the surface. $\boldsymbol{r}$ is the electron coordinate with respect to the surface, $\boldsymbol{D}(t)$ is the projectile–surface distance, and $\rho_{\boldsymbol{k}}$ the metal density of states.

We first perform the continuum discretization along the surface normal, by using a discrete sum of wave packets (so-called 'Weyl packets') instead of a continuum of jellium wavefunctions,

$$\int b_{\boldsymbol{k}}(t)\exp(-\mathrm{i}E_{\boldsymbol{k}}t)\phi_{\boldsymbol{k}}(\boldsymbol{r})\rho_{\boldsymbol{k}}\,\mathrm{d}\boldsymbol{k} \approx \sum_i \int_{A_i} b_{\boldsymbol{k}_\parallel,\bar{k}_{z_i}}(t)\exp(-\mathrm{i}E_{\boldsymbol{k}_i}t) \times \int_{\bar{k}_{zi}-\delta_z/2}^{\bar{k}_{zi}+\delta_z/2}\phi_{\boldsymbol{k}_\parallel,k_z}(\boldsymbol{r})\rho_{\boldsymbol{k}}\,\mathrm{d}\boldsymbol{k}_\parallel\,\mathrm{d}k_z, \qquad (2)$$

where 'i' labels the wave packets, $\boldsymbol{k}_i=(\boldsymbol{k}_\parallel,\bar{k}_{z_i})$, and $\bar{k}_{z_i}$ is the wave vector component perpendicular to the surface. The integration area in the $\boldsymbol{k}_\parallel$ space of momenta in the surface plane is given

by $A_i=\{\boldsymbol{k}_\parallel|k_\parallel^2+\bar{k}_{z_i}^2\le k_{\max}^2\}$, where $k_{\max}=\sqrt{2V}=1.077$ a.u. is the maximum momentum of the metal electrons, and $V=0.58$ a.u. is the energy of the bottom of the conduction band for an aluminum surface. The Weyl packets are obtained by superimposing jellium wavefunctions $\phi_{k_z}(z)$ with constant reflection and transmission coefficients $R(\bar{k}_{z_i})$ and $T(\bar{k}_{z_i})$ within a small momentum interval δ_z around the centroid momentum $\bar{k}_{z_i}$,

$$\phi_{\bar{k}_{z_i}}\approx\sqrt{\frac{\delta_z}{2\pi}}\left\{\frac{2\sin[(\delta_z z)/2]}{\delta_z z}\,[R(\bar{k}_{z_i})\exp(-i\bar{k}_{z_i}z)+\exp(i\bar{k}_{z_i}z)]\Theta(-z)+T(\bar{k}_{z_i})\exp(-\gamma z)\Theta(z)\right\}. \tag{3}$$

Fig. 1 shows examples for two different values of δ_z.

Next, we discretize the electron's motion in the surface plane by superimposing plane waves within small intervals δ_x and δ_y centered around the momenta $\bar{k}_{x_m}$ and $\bar{k}_{y_n}$:

$$\phi_{\bar{k}_{x_m}}(x)=\sqrt{\frac{\delta_x}{2\pi}}\,\frac{2\sin[(\delta_x x)/2]}{\delta_x x}\exp(i\bar{k}_{x_m}x),$$

$$\phi_{\bar{k}_{y_n}}(y)=\sqrt{\frac{\delta_y}{2\pi}}\,\frac{2\sin[(\delta_y y)/2]}{\delta_y y}\exp(i\bar{k}_{y_n}y). \tag{4}$$

Thus, we obtain a set of basis wave functions $\phi_{m,n,i}(\boldsymbol{r})=\phi_{\bar{k}_{xm}}(x)\phi_{\bar{k}_{yn}}(y)\phi_{\bar{k}_{zi}}(z)$ (where 'm', 'n' and 'i' label wave packets in the Ox, Oy and Oz directions), such that

$$\int b_k(t)\exp(-iE_k t)\phi_k(\boldsymbol{r})\rho_k\,d\boldsymbol{k}\approx\sum_{m,n,i}b_{m,n,i}(t)\exp(-iE_{m,n,i}t)\phi_{m,n,i}(\boldsymbol{r}). \tag{5}$$

The wavefunctions $\phi_{m,n,i}(\boldsymbol{r})$ are orthogonal, normalized, and localized near and in the surface due to the damping factors $[2\sin(\delta_\xi\xi/2)]/(\delta_\xi\xi)$, $\xi=x,y,z$.

The total Hamiltonian of the ion–surface system,

$$H=T+V_a+V_s+V_{as}, \tag{6}$$

includes the kinetic energy of the active electron T, the atomic Coulomb potential, screened inside the metal (r_p is the electron coordinate with respect to the atom)

$$V_a=-\frac{Q}{r_p}\,[\Theta(z)+\Theta(-z)\exp(-|z|/\lambda)], \tag{7}$$

the effective surface potential V_s (taken as a potential step at the jellium edge), and the atom–surface interaction V_{as}. Q designates the nuclear charge. V_{as} includes electronic and nuclear image potentials (the latter approximated by its values on the surface normal through the projectile nucleus), such that

$$V_s+V_{as}=\begin{cases}-V, & z<z_{\text{match}};\\ -\dfrac{1}{4(z-z_0)}+\dfrac{Q}{|D+z-2z_0|}, & z>z_{\text{match}}.\end{cases} \tag{8}$$

The image charge plane for the aluminum surface is located at $z_0=0.7$ a.u. [3]. The matching distance z_{match} guarantees the continuity of V_s+V_{as}, and the screening length inside the metal is taken as $\lambda=1$ a.u. Splitting the total Hamiltonian as $H=T+V_s+V_i$ and as $H=T+(-Q/r_p)+V_f$ allows us to identify the perturbation potentials in the initial and final charge transfer channels, $V_i=V_a+(V_s+V_{as})\Theta(z)$ and $V_f=(-Q/r_p)[\exp(-|z|/\lambda)-1]\Theta(-z)+V_s+V_{as}$, respectively. With the discretization (5), the expansion (1) now leads to a set of coupled equations. By numerically solving these equations for a given initial occupation, we obtain the time-dependent atomic and metallic population amplitudes a_j and $b_{m,n,i}$.

3. Results

We discuss results where the active electron's motion in the surface plane has been disregarded. We expect dominant contributions to the sums over 'm' and 'n' in Eq. (5) from metal electrons with parallel momenta contained in a small interval around $k_\parallel=0$, due to relatively large transmission coefficients T. To limit the computational effort in our first numerical application, we therefore restrict the expansion (5) to conduction-band

electrons contained in a thin cylinder of diameter δ_{par} inside the Fermi sphere. For $\delta_{par}=0.02$ a.u., i.e., for $|k_\parallel|\leq 0.02$, all transfer matrix elements are approximately constant.

We study the case of a $2p_0$-excited hydrogen atom at perpendicular incidence on an aluminum surface with speed $v_z=0.005$ a.u. This velocity is low enough in order to neglect translation factors in our calculations. By representing the atom–surface interaction in terms of a planar averaged Thomas–Fermi–Molière potential energy [11], we obtain the distance of closest approach (to the jellium edge) $d_{min}=3.5$ a.u. The following results are obtained using 160 metal Weyl packets and are converged with respect to the number of Weyl packets included.

Results for calculations including two atomic levels 2s and $2p_0$ in Eq. (1) are shown in Fig. 2, in parabolic representation of the hydrogen states [12,13]. These states mix strongly and form hybrids in front of the surface. A significant part of the hybridization near the surface corresponds to the 'Stark-like' mixing of spherical hydrogenic states in the non-uniform field of the surface [10]. For this reason their representation in the parabolic basis is more appropriate than in the spherical basis. In parabolic representation, the orbitals are described by the set of quantum numbers (n, k, m) where k is the 'electric' quantum number. For the two $n=2, m=0$ states, $k=-1$ $(+1)$ corresponds to the linear combination $\psi_{2s}+\psi_{2p_0}$ $(\psi_{2s}-\psi_{2p_0})$ of spherical hydrogenic orbitals. The squared amplitudes corresponding to the two $k=-1$ and $k=1$ orbitals and the sum of the squared amplitudes of all metal states are shown as a function of the atom–surface distance in Fig. 2. For ion–surface distances larger than 12 a.u. (region 1 in Fig. 2), the two states mix due to the interaction with the surface, but there is no charge exchange with the metal subspace. Below 12 a.u., in the second region (labeled by 2 in Fig. 2), the hydrogenic states mix strongly and begin to decay into the metal, as is seen by the increasing population density of the metal subspace. At large atom–surface distances on the outgoing

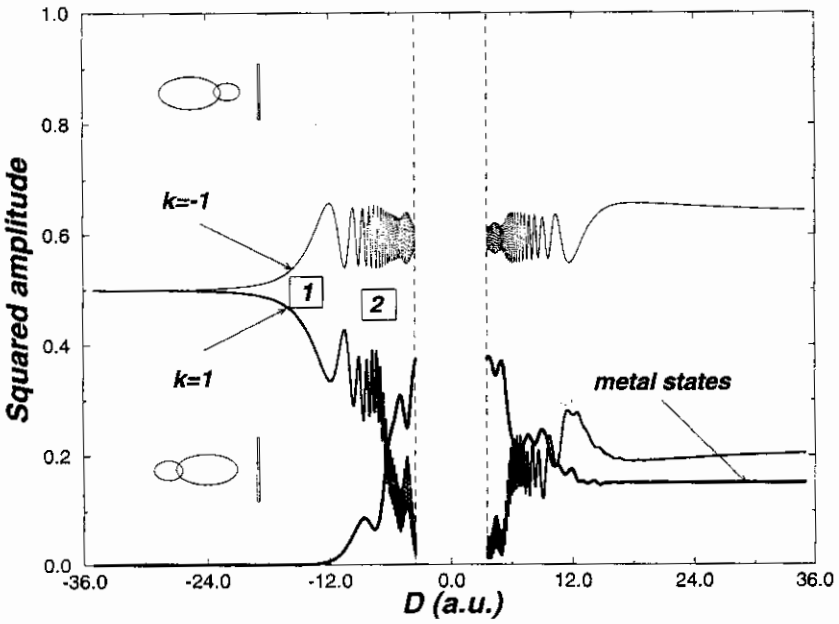

Fig. 2. Incident hydrogen atom, initially excited to $2p_0$ state, interacting with an aluminum surface at perpendicular incidence with speed $v_z=0.005$ a.u., in parabolic representation. Squared amplitudes as a function of the atom–surface distance D. Close-coupling calculation restricted to two atomic states (2s, $2p_0$) and 160 metal wave packets. Electric quantum numbers $k=-1$ and $k=1$ correspond to orbitals oriented away from and towards the surface. Insets show schematically the orientation of the Stark states.

trajectory, the atomic and metal amplitudes stabilize to constant values, which yield the final atomic and metal occupations after the collision. The coupling of the $k=-1$ state (with relatively small overlap with the surface) to the metal is weaker than for the $k=+1$ state (which has a relatively large overlap) and results in less charge transfer to the metal half space.

Fig. 3 shows the evolution of population amplitudes of the $n=2$ and $n=3$ manifolds in parabolic representation. The calculation includes all levels of the atomic $n\leq 5$ and $m=0$ manifolds. In contrast to Fig. 2, the results shown in Fig. 3 for the $n=2$ manifold are converged with respect to the number of atomic states included. On the incoming part of the trajectory, for distances larger than 18 a.u., 2s and $2p_0$ levels are unperturbed by the $n=3$ manifold (see region 1 in Fig. 2), but at about 18 a.u. the $n=3$ manifold becomes populated, hindering in this way the $n=2$ states from pure mixing. Electron transfer into the metal starts at about 12 a.u., i.e., at a distance lying between the classical threshold distances $D_{n=2}=8$ a.u. and $D_{n=3}=18$ a.u. [14]. On the outgoing trajectory, the population of the $n=2$ states stabilizes at about 20 a.u. The $k=1$ component vanishes, while 'Stark-like' mixing inside the $n=3$ manifold and interactions with other atomic states continue to change the populations in the $(n=3, m=0)$ subspace at 36 a.u. We find that it is sufficient to include the atomic $n=3$ and 4 manifolds in the close-coupling calculations, in order to obtain converged population amplitudes for the $n=2$ states.

4. Summary

A new close-coupling approach including continuum discretization has been developed to treat ion–surface interactions. In this model, the electron motion inside the metal is described by using Weyl wave packets. Couplings between the wave packets are explicitely included. In first numerical applications to hydrogen/aluminum collisions, we showed the evolution of the atomic and metallic population

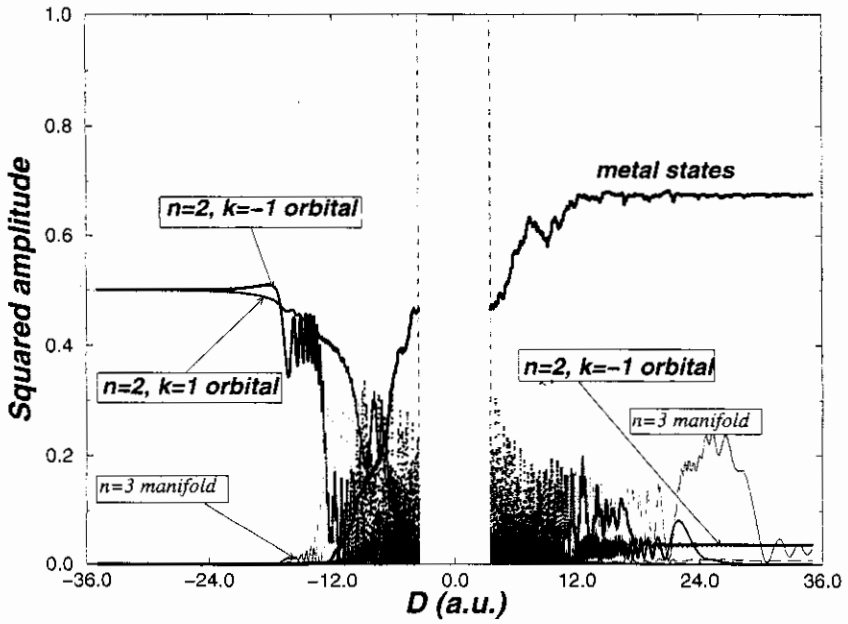

Fig. 3. Evolution of the squared amplitudes of the $n=2$, $k=-1$, $+1$ states, of all $n=3$ states, and of all 160 Weyl packets used to discretize the conduction-band continuum as a function of the atom–surface distance D. The calculation includes all $n\leq 5, m=0$ atomic basis states for excited hydrogen atoms at perpendicular incidence with speed $v_z=0.005$ a.u. on an aluminum surface.

amplitudes and discussed the main processes occuring during the collision.

Acknowledgements

This work was supported by NSF grant PHY-9604872. We also acknowledge partial support by the Division of Chemical Sciences, Office of Basic Energy Sciences, Office of Energy Research, US DOE, and the hospitality of the Institute for Theoretical Atomic and Molecular Physics at Harvard University and the Smithsonian Observatory.

References

[1] J.J.C. Geerlings, L. Los, Phys. Rep. 190 (1990) 133.
[2] J. Burgdörfer, in: C.D. Lin (Ed.), Review of Fundamental Processes and Applications of Atoms and Ions, World Scientific, Singapore, 1993.
[3] P. Kürpick, U. Thumm, U. Wille, Phys. Rev. A 56 (1997) 543.
[4] A. Arnau, F. Aumayr, P.M. Echenique, M. Grether, W. Heiland, J. Limburg, R. Morgenstern, P. Roncin, S. Schippers, R. Schuch, N. Stolterfoht, P. Varga, T.J.M. Zouros, H.P. Winter, Surf. Sci. Rep. 27 (1997) 113.
[5] P. Nordlander, J.C. Tully, Phys. Rev. B 42 (1990) 5564.
[6] D. Teillet-Billy, J.P. Gauyacq, Surf. Sci. 239 (1990) 343.
[7] S.A. Deutscher, X. Yang, J. Burgdörfer, Nucl. Instrum. Methods B 100 (1995) 336.
[8] F. Martin, M.F. Politis, Surf. Sci. 356 (1996) 247.
[9] V.A. Ermoshin, A.K. Kazansky, Phys. Lett. A 218 (1996) 99.
[10] P. Kürpick, U. Thumm, Phys. Rev. A 58 (1998) 2174.
[11] J.J. Ducrée, F. Casali, U. Thumm, Phys. Rev. A 57 (1998) 338.
[12] U. Thumm, P. Kürpick, U. Wille, Phys. Rev. B 61 (2000) 3067.
[13] D. Park, Z. Phys. 159 (1960) 155.
[14] U. Wille, Phys. Rev. B 50 (1994) 1888.